Studies on the Protein−Receptor Interaction by Atomic Force Microscopy

ARTICLE *in* LANGMUIR · NOVEMBER 2003

Impact Factor: 4.46 · DOI: 10.1021/la035391k

Studies on the Protein−Receptor Interaction by Atomic Force Microscopy

Srikanth Vengasandra, Gopi Sethumadhavan, Funing Yan, and Rong Wang*

Department of Biological, Chemical and Physical Sciences, Illinois Institute of Technology, Chicago, Illinois 60616

Received July 30, 2003. In Final Form: October 8, 2003

The specific interaction between a model biomolecular pair, cholera toxin B oligomer (CTB) versus its receptor ganglioside GM1, was investigated using an atomic force microscope. Force versus separation curves in approach/retraction cycles between a GM1-coated tip and CTB were collected. On the basis of a statistically significant number of force curves measured at different points on the sample surface, attractive forces during retraction were frequently observed. As confirmed by the results of control experiments, the attractive force was correlated to the rupture force of the CTB−GM1 specific bond, a quantitative measure of the specific interaction. Using a GM1-coated tip, force maps were generated on the CTB-containing surface to illustrate the CTB distribution. By varying the approach/retraction rate at 0.5, 1.0, and 3.0 Hz, the mean adhesive forces of 0.49, 0.17, and 0.03 nN were measured. It allows the quantification of the characteristic interaction time needed for strong CTB−GM1 binding in the range of 7−20 ms when CTB and GM1 were separated at a distance shorter than 10 nm. A shorter interaction time dramatically decreased the strength of the binding. We also observed a strong influence of the ionic strength on the binding time. The specific bond formation was significantly delayed in the presence of electrolyte in the media. This is ascribed to the influence of the ionic strength on both long-range and short-range interactions.

Introduction

Proteins are the fundamental biofunctional units. Biological function of a protein is mediated by its specific interaction with the receptor. The specific interaction is governed by the subtle interplay of a variety of forces such as hydrogen bonding, ionic bonding, van der Waals force, and hydrophobic interaction. An understanding of protein−receptor interactions is important to fields as diverse as drug development, disease diagnosis, and biosensing, among others. The relative strength of protein−receptor interactions can be estimated using the affinity constant, K_0,[1] the dissociation constant of the specific binding event. This parameter is a macroscopic measure of specific interaction and is generally determined using immunoassays,[2] surface plasma resonance,[3] and isothermal titration calorimetry.[4] However, none of these methods can be used to directly quantify the force strength of the protein−receptor interaction. Many new techniques and tools, such as optical tweezers, surface force apparatus, micropipets, and atomic force microscopy,[5] have been developed to directly measure the interaction between biomolecules. Because the binding force typically falls in the range of pico-Newtons to nano-Newtons and the size of a protein is on the nanometer scale, in our experiments we used the atomic force microscope (AFM) to study the protein−receptor interaction because of this tool's high spatial resolution and high sensitivity for force measurement.[6−9]

The AFM is a powerful tool for the examination of topographic features on sample surfaces. The potential of an AFM to directly measure intermolecular forces down to the 10 pN range was first highlighted by Hoh et al.[10] in an inorganic system. Various groups have exploited this technique to investigate specific recognition events between biomolecular pairs, for example, protein−receptor, antigen−antibody, and complementary oligonucleotides, in liquid under physiological conditions.[11−16] In a practical study of the protein−receptor interaction, the protein or receptor molecules are immobilized to an AFM tip. When the functionalized AFM tip approaches a surface with its countermolecules (receptor or protein), a specific bond forms between the biomolecular pair. As the tip retracts from the surface, a significant adhesive force will be observed in the force curve, quantitatively correspond-

* Corresponding author. Tel.: (312) 567-3121. Fax: (312) 567-3494. E-mail: wangr@iit.edu.

(1) Harlow, E.; Lane, D. *Antibodies: a Laboratory Manual*; Cold Spring Harbor Laboratory Press: Plainview, NY, 1988; pp 27−28.
(2) Chu, K. S.; Jin, G.; Guo, J. R.; Ju, M.; Huang, J. J. *Biotechnol. Prog.* **1995**, *11*, 352−356.
(3) Pellequer, J. L.; Vanregenmortel, M. H. V. *J. Immunol. Methods* **1993**, *166*, 133−143.
(4) Wiseman, T.; Williston, S.; Brandts, J. F.; Lin, L.-N. *Anal. Biochem.* **1989**, *179*, 131−137.
(5) Leckband, D. *Annu. Rev. Biophys. Biomol. Struct.* **2000**, *29*, 1−26 and references therein.
(6) Butt, H.-J.; Jaschke, M.; Ducker, W. *Bioelectrochem. Bioenerg.* **1995**, *38*, 191−201.
(7) Shao, Z.; Mou, J.; Czajkowsky, D. M.; Yang, J.; Yuan, J.-Y. *Adv. Phys.* **1996**, *45*, 1−86.
(8) Stoffler, D.; Steinmetz, M. O.; Aebi, U. *FASEB J.* **1999**, *13*, S195−S200.
(9) Dufrêne, Y. F. *Micron* **2001**, *32*, 153−165.
(10) Hoh, J. H.; Cleveland, J. P.; Pratter, C. B.; Revel, J.-P.; Hansma, P. K. *J. Am. Chem. Soc.* **1992**, *114*, 4917−4918.
(11) Florin, E.-L.; Moy, V. T.; Gaub, H. E. *Science* **1994**, *264*, 415−417.
(12) Moy, V. T.; Florin, E.-L.; Gaub, H. E. *Science* **1994**, *266*, 257−259.
(13) Hinterdorfer, P.; Baumgarter, W.; Gruber, H. J.; Schilcher, K.; Schindler, H. *Proc. Natl. Acad. Sci. U.S.A.* **1996**, *93*, 3477−3481.
(14) Allen, S.; Chen, X.; Davies, J.; Davies, M. C.; Dawkes, A. C.; Edwards, J. C.; Roberts, C. J.; Sefton, J.; Tendler, S. J. B.; Williams, P. M. *Biochemistry* **1997**, *36*, 7457−7463.
(15) Lee, G. U.; Kidwell, D. A.; Colton, R. J. *Langmuir* **1994**, *10*, 354−357. Lee, G. U.; Chrisey, L. A.; Colton, R. J. *Science* **1994**, *266*, 771−773.
(16) Wong, S. S.; Joselevich, E.; Woolley, A. T.; Cheung, C. L.; Lieber, C. M. *Nature* **1998**, *394*, 52−55.

10.1021/la035391k CCC: $25.00
Published on Web 11/25/2003

ing to the rupture force of the specific bond. This rupture force provides a measure of the strength of the specific interaction. When a receptor-modified tip scans a protein-present surface, a force map can be generated to illustrate the local distribution and association of the proteins.

The specific interaction between a protein−receptor pair is greatly influenced by environmental parameters, for example, electrolyte concentration[17,18] and molecular orientation.[19] Another important parameter is the protein−receptor interaction time. It is expected that a critical interaction time is required to allow formation of a strong specific bond. The present investigation looks into the dynamic behavior of protein−receptor interactions. We use the well-documented system of protein cholera toxin (CT) and its receptor ganglioside GM1 as a model system.[20−27]

CT is an oligomeric protein toxin composed of five identical B subunits and an A subunit ($M_r = 27$ kDa). The five B subunits (each of $M_r = 11.6$ kDa) form a pentamer with a central hole. It is the B subunits that are responsible for binding to receptors. The B pentamer binds strongly to ganglioside GM1 and also binds weakly to other gangliosides (about a 1000-fold weaker).[24] In this work, we studied the strength of specific binding of the cholera toxin B (CTB) subunit to GM1. We first characterized the CTB structure with high-resolution images. The CTB−GM1 specific interaction was probed using force curves and force maps. Conditions for forming strong specific bond were examined by minimizing the interaction time. The stronger the specific binding, the higher is the sensitivity for detecting the proteins. This was revealed by the effect of electrolyte on the binding event.

Experimental Section

Materials. Succinimidyl-3,2-(2-pyridyldithio)propionate (SPDP) was purchased from Molecular Probes (Eugene, Oregon). An SPDP solution of 1.64×10^{-4} M was prepared by dissolving SPDP in *N*,*N*-dimethylformamide (DMF). Lyso-monosialoganglioside GM1 was supplied by Matreya, Inc. (Pleasant Gap, PA). A 7.71×10^{-5} M solution was prepared in DMF, ready for the reaction with SPDP to covalently bind the GM1 to a gold-coated AFM tip. Phosphate buffered saline (PBS) with pH 7.4 and CTB oligomer were purchased from Sigma-Aldrich Co. CTB was dissolved in a 0.01 M PBS solution to achieve a final concentration of 1.4×10^{-7} M.

Silicon Substrate Modification with CTB. We functionalized CTB onto a silicon wafer using thiol−gold chemistry with a cross-linker, as reported by others[19,28] and as routinely performed in our lab.[29] In brief, 10 nm-titanium and 100-nm gold were subsequently deposited onto a silicon wafer using an electronic-beam evaporator (Therminonics, Inc., Hayward, CA). The substrates were ultrasonicated with acetone and ethanol to remove any traces of surface impurities. After being thoroughly dried, a gold-coated substrate was immersed into a SPDP solution for 12 h at room temperature under N_2 gas protection, allowing the covalent bonding of a monolayer of SPDP onto the gold substrate via thiol−gold linkage. The modified substrate was rinsed with DMF several times to remove the unbounded residues from the surface. The substrate was then immersed in the CTB/PBS solution overnight at room temperature under N_2 protection. The succinimidyl group of SPDP is reactive to the amino acid groups on CTB.[19,28,29] Thus, the SPDP functions as a cross-linker to anchor the CTBs onto the gold substrate. Successful modification was confirmed with AFM images. It was also confirmed using the force measurements via the GM1 functionalized tip. A reasonably stable adhesive force was reproducibly observed in the tip-retraction process.

AFM Tip Functionalization with GM1. Functionalization of ganglioside GM1 onto a gold-coated AFM tip was slightly different. A total of 200 μL of 7.71×10^{-5} M lyso-GM1 in a DMF solution was added into 150 μL of a 1.64×10^{-4} M SPDP solution. The mixture was diluted to 5 mL and kept overnight (>12 h) at room temperature under N_2 protection. During this step, the amino group of lyso-GM1 reacted with the succinimidyl group of SPDP to form an amide. Again, the SPDP served as a cross-linker to immobilize the GM1 molecules onto an AFM tip, which was precoated with 3-nm titanium and 50-nm gold. The AFM tip was then rinsed with DMF, which ensured the removal of any loosely bound GM1 molecules. The functionalized tip was kept in pure water until use.

Atomic Force Microscopy. This study was carried out with a multimode Nanoscope IIIa AFM (Digital Instruments, Santa Barbara, CA). The images were acquired in the fluid-tapping mode using oxide sharpened Si_3N_4 tips in a 0.01 M PBS solution, operating at a thermal resonance frequency of 8−10 kHz.

The force plots were obtained in the fluid-contact mode. As shown in Figure 1, CTB and its receptor GM1 were immobilized onto a substrate and an AFM tip, respectively (Figure 1a). As the GM1-modified tip approached the CTB-containing surface, a specific bond formed (Figure 1b); meanwhile, the tip experienced repulsion due to contact forces, as illustrated in Figure 1c. As the tip was retracted from the surface, an attractive force due to the rupture of the specific bond between CTB and GM1 was detected, providing a quantitative measure of the specific interaction. To achieve a force−volume (FV) image, a 1 μm × 1 μm area of the CTB-containing surface was scanned using the GM1-functionalized tip, and a total of 32 × 32 force curves were collected to generate the force map. The rate with which the tip approached and retracted from the substrate was varied to study the dynamic properties of the specific binding.

The spring constant of the cantilever was calibrated in the air-tapping mode following the standard procedure available via the Nanoscope IIIa software. The spring constant of the triangular cantilever that we used for force measurements was calibrated to be 0.07 nN/nm within an error range of 25%. Force measurements were performed in a 0.01 M PBS solution in a fluid cell unless particularly noted in the text.

Results

Images of CTB on a Silicon Wafer and a Au Substrate. Because the surface of a silicon wafer is negatively charged whereas CTB has a net positive charge,[30] the electrostatic interaction enables the physisorption of CTBs on the silicon wafer. Figure 2 shows a sequence of three-dimensional images collected on a silicon wafer after incubation with the CTB solution for 1 h. The sample was thoroughly rinsed with a PBS solution prior to imaging. In Figure 2a, tiny bright spheres are uniformly and densely distributed across the 756 nm × 756 nm surface area. Large bright features, corresponding to clusters of CTB molecules, occasionally appear on the surface. In the higher resolution image (Figure 2b), the size of an individual bright sphere is determined to be 5.6 ± 0.4 nm in diameter and 2.6 ± 0.3 nm in height with

(17) Rotsch, C.; Radmacher, M. *Langmuir* **1997**, *13*, 2825−2832.
(18) Smith, D. A.; Wallwork, M. L.; Zhang, J.; Kirkham, J.; Robinson, C.; Marsh, A.; Wong, M. *J. Phys. Chem. B* **2000**, *104*, 8862−8870.
(19) Harda, Y.; Kuroda, M.; Ishida, A. *Langmuir* **2000**, *16*, 708−715.
(20) Cuatrecasas, P. *Biochemistry* **1973**, *12*, 3547−3565.
(21) Fishman, P. H.; Moss, J.; Osborne, J. C., Jr. *Biochemistry* **1978**, *17*, 711−716.
(22) Goins, B.; Freire, E. *Biochemistry* **1988**, *27*, 2046−2052.
(23) Zhang, R.-G.; Westbrook, M. L.; Westbrook, E. M.; Scott, D. L.; Otwinowski, Z.; Maulik, P. R.; Reed, R. A.; Shipley, G. G. *J. Mol. Biol.* **1995**, *251*, 550−562.
(24) Kuziemko, G. M.; Stroh, M.; Stevens, R. C. *Biochemistry* **1996**, *35*, 6375−6384.
(25) Yang, J.; Tamm, L. K.; Tillack, T. W.; Shao, Z. *J. Mol. Biol.* **1993**, *229*, 286−290.
(26) Mou, J.; Yang, J.; Shao, Z. *J. Mol. Biol.* **1995**, *248*, 507−512.
(27) Czajkowsky, D. M.; Shao, Z. *FEBS Lett.* **1998**, *430*, 51−54.
(28) Dammer, U.; Hegner, M.; Anselmetti, D.; Wagner, P.; Dreier, M.; Huber, W.; Güntherodt, H.-J. *Biophys. J.* **1996**, *70*, 2437−2441.
(29) Wang, R.; Vengasandra, S.; Yan, F. *Chem Lett.* **2001**, *11*, 1170−1171.
(30) Luckham, P. F.; Smith, K. *Faraday Discuss.* **1998**, *111*, 307−320.

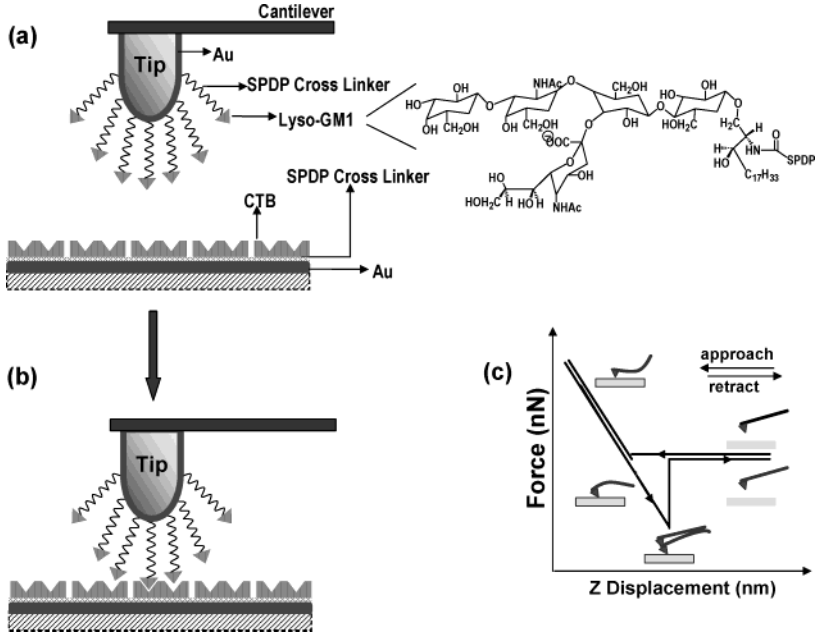

Figure 1. Schematic illustrations of a GM1-modified AFM tip and a CTB-modified Si substrate (a), the CTB−GM1 binding event upon tip approach (b), and the force curves during tip approach and retraction (c).

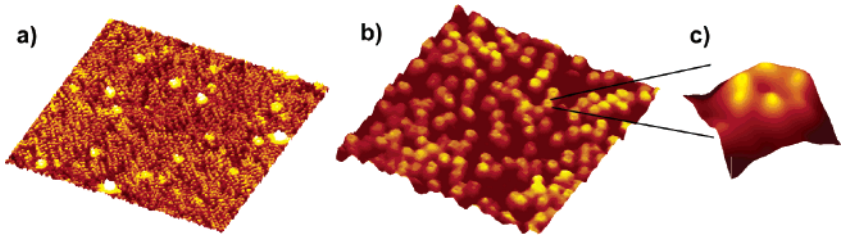

Figure 2. Sequence of three-dimensional height images collected on a Si wafer after incubation with a CTB solution of 1.4×10^{-7} M in PBS for 1 h. Sizes of the images are (a) 756 × 756, (b) 146 × 146, and (c) 8 × 8 nm^2.

respect to the blank areas (dark regions in the image), which is characteristic for a CTB molecule. The measured size is in good agreement with our previous report[29] as well as with other AFM research[25−27] and an X-ray crystallographic study.[23] The zoom-in image in Figure 2c resolves the five B subunits of an individual CTB along with a central pore of 1.7 ± 0.3 nm across. The submolecular resolution images of CTB were reproducibly achieved on mica and gold-coated substrates (see subsequent text).

To study the binding affinity between CTB and GM1, CTB and GM1 molecules were covalently bound to a gold-coated silicon wafer and a gold-coated AFM tip, respectively, using the SPDP cross-linker as delineated in the Experimental Section. The strong covalent linkage ensured a solid fixation of proteins and receptors to the surfaces, so that the specific interaction could be measured between the tip and the sample during the tip-approach/retraction cycle. The CTB functionalized substrate was initially characterized using a bare Si_3N_4 tip, as shown in Figure 3. Compared with the image of a pure gold substrate (not shown), the flat patches encircled by dark curvy boundaries are identified as gold islands with an approximate size ranging from 200 to 500 nm. On top of the gold islands, densely and uniformly distributed bright spheres are evident. These spheres show a relative height of 2.8 ± 0.3 nm, confirming the successful immobilization of a monolayer of CTB on the gold substrate. Beside the CTB monolayer, large and high features are observed at the gaps of gold islands, as shown in Figure 3. Most likely, the CTB clusters were accumulated on the bare substrate. The characteristic pentameric structure of CTB was

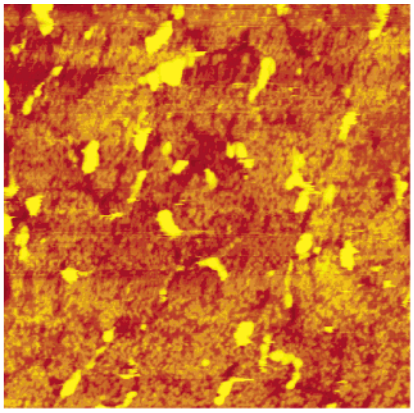

Figure 3. 2 × 2 μm^2 height image of CTBs covalently linked to a gold-coated Si substrate. See Experimental Section for sample preparation.

resolved for the individual bright sphere in high-resolution images similar to that of Figure 2c. In any 1 μm × 1 μm section of the substrate, the monolayer distribution of CTB was dense and analogous. This allowed us to randomly sample any 1 μm × 1 μm section of the substrate for a meaningful statistical analysis of the CTB−GM1 specific interaction.

Force Measurement between a GM1-Modified Tip and a CTB-Modified Substrate. GM1 was functionalized on an AFM tip in a very similar way. The use of lyso-GM1 for tip modification ensured that the polysaccharide binding sites extended out and were available for binding to CTB. The successful functionalization of the

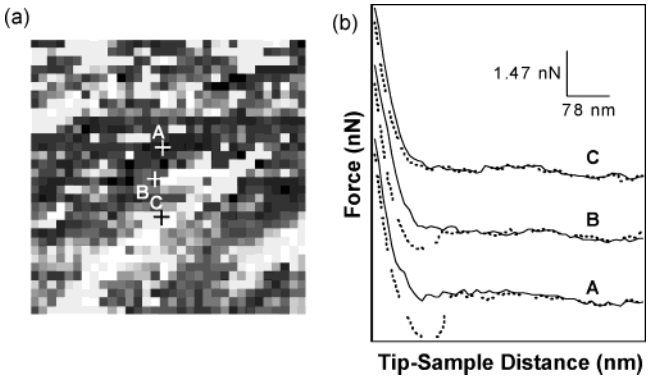

Figure 4. (a) $1 \times 1\ \mu m^2$ FV image acquired between a GM1-functionalized tip and a CTB-modified surface at a *Z*-scan rate of 0.5 Hz and a *Z*-ramp size of 500 nm. (b) Force curves collected at the sample data points as marked in part a. Solid lines, tip-approach traces; dashed lines, tip-retraction traces.

tip and the substrate is evident from the reproducible and stable adhesive forces measured between the modified tip and the substrate at local regions. In contrast, when force curves were measured between a tip with physisorbed GM1 and a substrate with chemically bound CTB or vice versa, high adhesive forces that were initially observed on a frequent basis quickly dropped to noise level in the subsequent force measurement cycles when the measurements were performed in the same region, indicative of the detachment of weakly bound species. These experiments confirmed both the successful surface functionalization and the retained affinities of the protein and receptor after chemical bonding.

The binding affinity between GM1 and CTB was quantified by force curves generated using FV imaging. Figure 4a shows a FV image acquired between a GM1-modified AFM tip and a CTB-modified surface. At each pixel on the image, the tip approached and retracted from the surface to complete a force curve measurement, as schematically illustrated in Figure 1c. As the tip scanned the surface, a total of $32 \times 32 = 1024$ force curves were collected to generate the FV image. When compared with 512×512 pixels in regular images with an unmodified tip, the resolution of a FV image is low because of the limitation of memory. In compensation, information of the tip−sample interaction at each pixel is available. The contrast in a FV image reflects the relative strength of the tip−sample interaction in the local region. The sampling frequency (*Z*-scan rate) was initially chosen to be 0.5 Hz; that is, the complete cycle of tip approach and retraction occurred in 2 s. The *Z*-ramp size, the distance the cantilever traveled in both the approach and the retraction processes, was 500 nm.

Figure 4b shows three typical force curves collected at the sample data points A, B, and C, as marked in the FV image in Figure 4a. When the GM1-coated tip approached the CTB surface, a net repulsive force was observed in all three force curves due to the repulsive steric interaction between the molecular pair.[15] During retraction, however, a strong attractive force of 1.45 nN was observed at A, corresponding to the darkest contrast in the FV image, whereas a relatively weaker force of 0.73 nN was measured at B, with a relatively lighter contrast in the FV image; the force curve of the brightest spot (C) shows no attractive peak above the noise level. These attractive forces quantitatively correlate to the rupture of the CTB−GM1 specific bonds.[5,7] The adhesive forces obtained over the entire sampled area vary, as indicated by the contrast in the FV image, and were in the range of 0−1.45 nN. A histogram of the percentage occurrence (frequency) of the

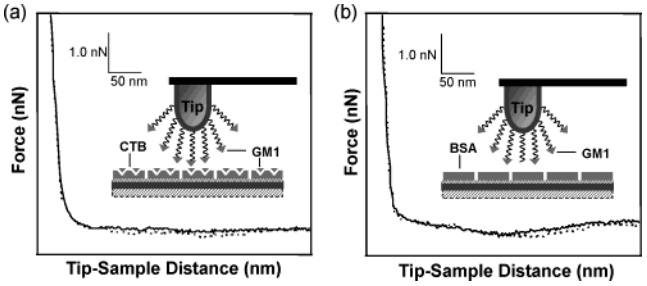

Figure 5. (a) Force curves collected between a GM1-modified tip and a CTB-functionalized substrate, where the CTB-functionalized substrate was pretreated by the GM1 solution. (b) Force curves collected between a GM1-modified tip and a BSA-functionalized substrate. Solid lines, tip-approach traces; dashed lines, tip-retraction traces.

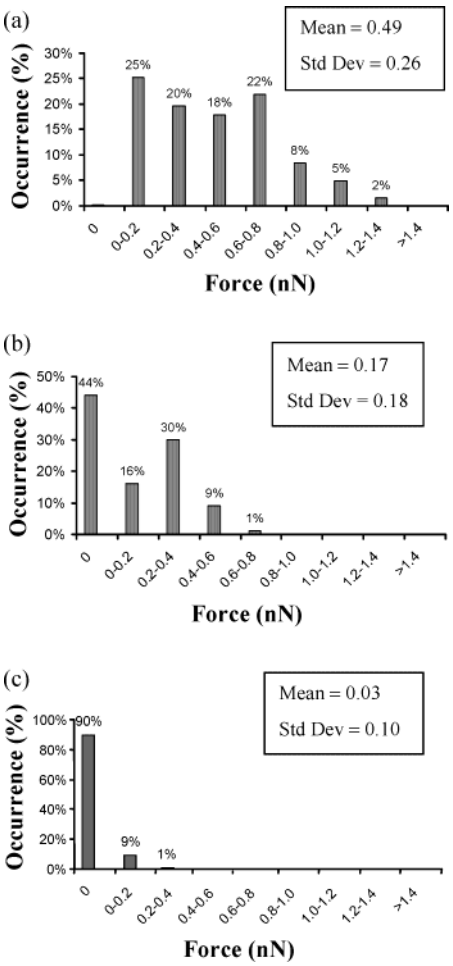

Figure 6. Histograms of maximum attractive force as a function of the frequency of occurrence, summarized from 1024 data points in FV images collected at *Z*-scan rates of (a) 0.5, (b) 1.0, and (c) 3.0 Hz. All the measurements were performed between the same GM1-functionalized tip and the same CTB-modified surface in a 0.01 M PBS solution. Mean attractive force (Mean) and corresponding standard deviation (Std Dev) are in nN.

adhesive forces is plotted in Figure 6a. The distribution has a mean attractive force of 0.49 nN and a standard deviation of 0.26 nN. The maximum attractive force that we detected is 1.45 nN.

In one control experiment, sufficient GM1 solution was applied to a CTB-functionalized substrate prior to the force measurement with a GM1-functionalized tip. As a result, the force curves exhibit analogous repulsive regimes in both the approach and the retraction curves, suggesting

Table 1. Adhesion Forces between CTB and the Functionalized/Bare AFM Tip

tip type/media	Z-scan rate (Hz)	mean force[a] (nN)	std dev[b] (nN)
GM1−tip/PBS	0.5	0.49	0.26
GM1−tip/PBS	1.0	0.17	0.18
GM1−tip/PBS	3.0	0.03	0.10
GM1−tip/pure water	1.0	0.46	0.37

[a] The mean force is defined as the average of the maximum adhesive forces measured. [b] std dev stands for the standard deviation of the maximum adhesive forces.

that the binding sites of CTB were completely blocked by the GM1 molecules in the solution phase, so that no reactive site was available for binding to the GM1 molecules on the tip. Figure 5a shows typical force curves collected under this condition. In this case, the detectable adhesive force (among more than 100 force measurements) during tip retraction was less than 0.02 nN. We also functionalized a gold-coated substrate with bovine serum albumin (BSA). The highest adhesive force (among more than 100 force measurements) detected between a GM1-modified tip and the BSA surface was 0.03 nN, negligible when compared with the CTB−GM1 interaction. Typical force curves are shown in Figure 5b. Essentially, minimum adhesion was obtained in both cases. The results of the control experiments provide strong evidence that the attractive forces acquired in Figure 4 were generated from the CTB−GM1 specific interaction.

Force Measurement at Various *Z*-Scan Rates. To investigate the characteristic time needed to form strong specific bonds, FV images (similar to that of Figure 4a) were also collected at *Z*-scan rates of 1.0 and 3.0 Hz using the same GM1-modified tip at the same region as that in Figure 4a. The *Z*-ramp size was maintained at 500 nm. The forces measured from 1024 data points in the FV image are summarized in the histograms in Figure 6b,c. At the higher *Z*-scan rate of 3.0 Hz, the GM1-modified tip hardly registered any attractive force (Figure 6c). As the *Z*-scan rate decreased to 1.0 Hz, the mean attractive force increased to 0.17 nN and the maximum attractive force detected was 0.80 nN (Figure 6b). A further decrease of the *Z*-scan rate to 0.5 Hz greatly enhanced the magnitude of the measured force (Figure 6a). It was also observed that multiple attractive peaks more frequently appeared at the lower *Z*-scan rate; consequently, the force distribution was broader. The dependence of the adhesive force on the *Z*-scan rate is summarized in Table 1. It is remarkable to observe that the magnitude of the measured force changed dramatically as the *Z*-scan rate varied in the narrow range of 0.5−3.0 Hz.

Influence of Media on the Magnitude of the Adhesive Force. All the data reported previously were obtained in a PBS solution at a pH of 7.4 (ionic strength of 0.17 mol/kg). Replacing the PBS with deionized water, an FV image was acquired at a *Z*-scan rate of 1.0 Hz over a 1 μm × 1 μm scan area. In a striking contrast to the low forces measured in the PBS solution, the adhesive forces were remarkably higher in deionized water. The adhesive force histogram (Figure 7) collected from the FV image indicates that the mean force in deionized water (0.46 nN) is approximately 3 times higher than the mean force in the PBS solution under similar conditions and that the force distribution is broader.

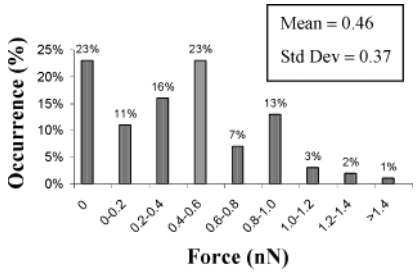

Figure 7. Histogram of the maximum attractive force as a function of the frequency of occurrence, summarized from 1024 data points in FV images collected between a GM1-functionalized tip and a CTB-modified surface in pure water, at a *Z*-scan rate of 1.0 Hz.

Discussion

Probing the CTB Distribution via the CTB−GM1 Specific Binding Event. Specific binding is known to occur between proteins and receptors and is generally believed to be mediated mainly by hydrogen bonds, ionic bonds, van der Waals bonds, and hydrophobic interactions.[5] In the CTB−GM1 system, one CTB can bind to a maximum of five GM1 receptors, and the corresponding binding force was quantified at 0.1 nN,[29,30] 1/20 of the strength of a typical covalent bond.[31] Thus, the covalent linkage of the protein (or the receptor) to a Si wafer (or an AFM tip) ensures that the rupture forces measured in the tip-approach/retraction cycle correlate to the specific interaction between the biomolecular pair.

In the present study, adhesive forces as low as 0.15 ± 0.5 nN were frequently observed regardless of the *Z*-scan rate (Figure 6). Considering that the measured forces at distinct data points are roughly multiples of this value and also considering the errors arising from the force measurements, we estimate that the CTB−GM1 specific interaction falls in the range of 0.1−0.2 nN. High-resolution images in Figure 2 indicate that the diameter of a CTB molecule is 5.6 nm; thus, the lateral area occupied by a single CTB molecule is approximately 25 nm^2. According to the SEM image of the gold-coated Si_3N_4 tip, the nominal tip radius is approximately 15 nm. Because the cross-sectional area of a GM1 molecule is ∼1 nm,[2,32] sufficient GM1 molecules are immobilized on top of the tip via self-assembly. As a result of the remarkable size difference between CTB and GM1, the local concentration of GM1 is much higher than the local concentration of CTB. Because the GM1 molecules were tethered to the tip via flexible chains, the high affinity between GM1 and CTB may have allowed the GM1 molecules to equally reach the five binding sites of each CTB pentamer. Thus, the 0.1−0.2 nN adhesive force more likely correlates to the interaction between a CTB and five GM1 molecules, which is consistent with the report by Luckham et al.[30] and our previous observation.[29] Because the CTBs are uniformly and densely distributed on the substrate (Figures 2 and 3), it is most likely that the specific bonds form between multiple CTBs and GM1s as the GM1-modified tip approaches the CTB-modified substrate, if sufficient interaction time is provided. This hypothesis is consistent with the broad distribution in the magnitude of rupture forces, as shown in the histogram in Figure 6a. The greater attractive force reveals a binding of more CTBs with the GM1-functionalized tip, indicative of a higher concentration of CTB at the local region and vice versa. The measured forces are characteristic for the CTB−GM1 specific interaction, confirmed by the measurement of greatly reduced force in the control experiments.

(31) Lantz, M. A.; Hug, H. J.; Hoffmann, R.; van Schendel, P. J. A.; Kappenberger, P.; Martin, S.; Baratoff, A.; Guntherodt, H.-J. *Science* **2001**, 2580−2583.

(32) Luckham, P.; Wood, J.; Froggatt, S.; Swart, R. The surface properties of gangliosides. *J. Colloid Interface Sci.* **1993**, *156*, 164−172.

The relative force contrast in the FV image in Figure 4a reflects the relative strength of the CTB−GM1 interaction, providing an approach to probing the protein distribution at local regions: strong attractive forces are generated at the dark regions, where CTB is highly concentrated; whereas the bright regions correlate to minimal forces and, thus, a lack of CTB. The results reveal that it is the GM1 molecules on the tip that register the locations of CTBs on the surface and that it is the specific interaction that enables the investigation of the protein distribution at local areas. Knowledge of protein distribution is important in understanding the protein function.

The same methodology was adapted to study the distribution of the nerve growth factor (NGF) receptor, TrkA, on the membrane of a PC12 living cell. TrkAs were identified on the cell membrane, and their local aggregation nature was revealed using FV images. This provided essential information when investigating the function of NGF in the nerve cell. This work will be reported separately.

Dynamic Properties of the CTB−GM1 Interaction. Protein−receptor interactions are governed by both long-range interactions and short-range interactions.[5] The dominant long-range interaction is the electrostatic interaction in terms of Derjaguin−Landau−Verwey−Overbeek (DLVO) force. The effective range of the long-range interaction is less than 10 nm. Because CTB is positively charged, it electrostatically attracts the negatively charged GM1 over a long range.[30] At a short range (less than 1−2 nm), the CTB−GM1 interaction is in large part formed from hydrogen bonds between juxtaposed complementary functional groups.[24]

The formation of specific bonds requires a certain interaction time. This can be understood from the histogram shown in Figure 6. It should be pointed out that the FV images at *Z*-scan rates of 0.5, 1.0, and 3.0 Hz were collected with the same GM1-modified tip at the same area of the CTB-modified surface. Thus, the histograms (Figure 6a−c) summarized from these force maps are comparable. In this study, the tip-approach and -retraction rates are the same, and there is no delay time between tip approach and tip retraction. The 3.0-Hz scan rate gives rise to a constant tip-approach/retraction rate of 3 nm/ms as the GM1-modified tip travels 500 nm to or from the CTB-modified surface. Assuming that the CTB−GM1 interaction is effective at a separation of less than 10 nm (accounting for both the long-range and the short-range interactions), the time that CTB and GM1 are held at this range during tip approach and retraction is less than 7 ms at the 3.0-Hz *Z*-scan rate. A total of 90% of the measured forces are 0. The most probable nonzero force is in the range of 0−0.2 nN. This is consistent with the fact that the interaction time is too short to allow multiple CTB−GM1 interactions. The lack of detected attractive forces indicates that 7 ms is the least amount of time required for the formation of a specific bond. As the time is increased to 20 ms (for a *Z*-scan rate of 1.0 Hz), notable attractive forces were detected as a result of specific bond formation (Figure 6c). A further decrease of the *Z*-scan rate (0.5 Hz) allows a longer time (40 ms) for the CTB−GM1 interaction within the 10-nm separation; hence, multiple bindings between CTB and GM1 molecules are more efficient, giving rise to a broad distribution of attractive forces. Note that bindings between multiple CTB and GM1 molecules are possible at any *Z*-scan rate because of the size of the AFM tip (15-nm nominal tip radius). However, multiple bindings are most frequently observed when a longer interaction time is provided.[33] This can be considered in the following way: an individual GM1 molecule orients randomly with respect to the binding sites of CTB immobilized on the substrate; as the GM1-modified tip approaches a CTB-modified surface, the fastest CTB−GM1 binding happens between the two molecules whose binding sites initially face each other. Only when the interaction time is sufficient, GM1 molecules with other orientations may adjust their orientations toward the binding sites of CTB via the flexible cross-linker so that multiple specific bonds are able to form. Our results indicate that a strong CTB−GM1 specific bond can form when the interaction time is 7−20 ms at a separation of less than 10 nm. This time scale may include the time for adjustment of the GM1 molecular orientation, diffusion to binding sites of CTB, and binding to CTB, as is discussed in detail below.

In a natural environment, the hydrophobic acyl chains of GM1 insert into the outer leaflet of the cell membranes, with the polysaccharide binding sites pointing out and available for binding to CTB in body fluid. When binding happens, the polysaccharide group of GM1 reaches the binding site of CTB in the deep pocket via long-range and short-range interactions. In our model system, both GM1 and CTB were immobilized. GM1 was anchored onto an AFM tip through a flexible cross-linker and, thus, largely retained the flexibility and mobility of the polysaccharide headgroup needed for efficient binding. On the other hand, rigid CTB molecules were fixed on the substrate. Because free CTB can facilitate the binding event, the actual interaction time must be shorter than that we determined in the model system. Our study identifies the lower limit for the interaction time.

It should be noted that a specific bond forms during the tip-approach process. However, in the AFM study, the strength of the bond between biomolecular pairs is estimated by the rupture force, that is, the external force applied to induce bond dissociation, which is measured during the tip-retraction process. Because dissociation is a consequence of bond formation, it is reasonable to use the rupture force to estimate the strength of bond formation if the bond dissociation is independent of the rupture force. Bell[34] first pointed out in 1978 that the bond dissociation rate between a ligand and its receptor should increase if an external force is applied to pull the bounded complex apart. It was recently confirmed experimentally that the external force effectively reduces the energy barrier for bond dissociation[35,36] and the increase in the tip-retraction rate over 6 orders of magnitude leads to an increase in the measured mean rupture force (which becomes 34 times higher).[35] However, in our experiment, we choose a retraction rate in the narrow range of 0.5 nm/ms (0.5-Hz scan rate) and 3 nm/ms (3.0-Hz scan rate) and the Bell effect is negligible. Experimentally, we observed an increase in the mean rupture force with the decrease of the *Z*-scan rate. This can be interpreted as an increase of interaction time with the decrease of the *Z*-scan rate, resulting in a reinforcement of the multiple binding as delineated previously. A longer interaction time (low *Z*-scan rate) allows the formation of a strong CTB−GM1 specific bond. Hemmerlé

(33) Zhang, X.; Wojcikiewicz, E.; Moy, V. T. *Biophys. J.* **2002**, *83*, 2270−2279.
(34) Bell, G. I. *Science* **1978**, *200*, 618−627.
(35) Merkel, R.; Nassoy, P.; Leung, A.; Ritchie, K.; Evans, E. *Nature* **1999**, *397*, 50−53.
(36) Gergely, C.; Voegel, J.-C.; Schaaf, P.; Senger, B.; Maaloum, M.; Hörber, J. K. H.; Hemmerlé, J. *Proc. Natl. Acad. Sci. U.S.A.* **2000**, *97*, 10802−10807.

et al.[37] drew a similar conclusion in their study of fibrinogen adhesion on a hydrophilic surface.

Alteration of the Binding Rate by Electrolyte. The ionic strength of the media alters the binding rate. Comparing Figure 7 with Figure 6b, the replacement of PBS with deionized water remarkably enhances the binding event. The mean force of Figure 7 at a 1.0-Hz scan rate was at the same level as that of Figure 6a, where the scan rate was 0.5 Hz. The broad force distribution implies that multiple binding occurred in a shorter interaction time in the absence of electrolyte. Thus, the absence of electrolyte in the medium accelerates the specific bond formation. The time required to form a specific bond in our current study is tentatively correlated to the following steps: (1) as the AFM tip brings the GM1 molecules close enough to the CTB-modified substrate, long-range electrostatic interaction becomes effective and dominant, causing the diffusion of GM1 toward the CTB binding sites[38] via the flexible linker; and (2) GM1 diffuses while adjusting the orientation to optimize its interaction with CTB mediated by short-range interactions (mainly hydrogen bonding in the case of the CTB−GM1 interaction).

The influence of electrolyte on the long-range CTB−GM1 interaction can be explained by the DLVO theory.[39] Electrostatic interaction arises when the electrical double layers of the interacting species overlap. This occurs at separations of a few tens of nanometers. The electrostatic component of the DLVO force increases with the thickness of the electric double layer, λ_D, defined as the Debye length.[39] Because λ_D is inversely proportional to the square root of ionic strength, the higher ionic strength in the PBS (0.17 mol/kg) versus deionized water gives rise to a lower electrostatic interaction. Computer simulation and mutagenesis studies have suggested that long-range intermolecular attractive forces may enhance association rates.[40,41] This enhancement is attributed to not only the reduction of the potential energy barrier of the collision but also the improved orientation of biomolecular trajectories.[42] In the absence of electrolytes, the relatively stronger attractive force reinforces the diffusion rates, lowers collision barriers, and, thus, aids in specific binding at much shorter interaction times. Accordingly, the presence of electrolytes requires a longer interaction time for the formation of a specific bond.

At short range, hydrogen bonding between the complementary functional groups of CTB and GM1 is essential in the specific interaction.[24] The small ions in the electrolyte create a strong electric field that can distort the hydrogen bond configurations[43] and in turn delay the specific binding event. Thus, when electrolyte is present in the medium, both long-range interactions and short-range interactions require a longer time for bond formation. This is consistent with our observations (Figures 6 and 7). The change in the ionic strength may also induce conformational changes of CTB and GM1, causing the change in the rate of specific interaction. However, there is currently no direct evidence to address this possibility.

Because living cells dictate the most efficient specific binding events in a natural environment, our study opens up a topic: though various ionic species exist in body fluid, the ionic strength near the cell membrane may be relatively low to optimize the specific interactions between cell surface receptors and their ligands. This topic will be explored in our future study of living cells.

Summary

We have used an AFM to investigate the specific recognition event between CTB and its receptor GM1. CTB immobilization and submolecular structure were characterized using high-resolution images. GM1-modified tips were used to detect the local distribution of CTB on a substrate. This approach can be easily adapted to any other biocomplementary system. By varying the tip-approach/retraction rate, we determined that a strong CTB−GM1 specific bond can form when the interaction time is 7−20 ms at a separation of less than 10 nm. This time scale includes the time that the GM1 molecules diffuse to the CTB binding sites via long-range electrostatic interaction, as well as the time that GM1 molecules reorient to optimize their interaction with CTB (mediated mainly by short-range hydrogen bonding). Both the electrostatic interaction and the hydrogen bonding are delayed by the presence of electrolyte in the medium, leading to a delay in specific bond formation.

Acknowledgment. This work was supported by NSF (IBN-0103080)). The authors thank Dr. M. Mrksich and Dr. J. Smith for their help with gold deposition and Dr. J-C. Voegel for valuable comments on the manuscript.

LA035391K

(37) Hemmerlé, J.; Altmann, S. M.; Maaloum, M.; Hörber, J. K. H.; Heinrish, L.; Voegel, J.-C. *Proc. Natl. Acad. Sci. U.S.A.* **1999**, *96*, 6705−6710.

(38) Wang, R.; Shi, J.; Parikh, A. N.; Shreve, A. P.; Chen, L.; Swanson, B. *Colloids Surf., B*, in press.

(39) Israelachvili, J. N. *Intermolecular and Surface Forces*, 2nd ed.; Academic Press, Ltd.: London, 1992.

(40) Wendoloski, J. J.; Matthew, J. B.; Weber, P. C.; Salemme, F. R. *Science* **1987**, *238*, 794−797.

(41) Stayton, P. S.; Sligar, S. G. *Biochemistry* **1990**, *29*, 7381−7386.

(42) Leckband, D. E.; Israelachvili, J. N.; Schmitt, F. J.; Knoll, W. *Science* **1992**, *255*, 1419−1421.

(43) Xu, H.; Berne, B. J. *J. Phys. Chem. B* **2001**, *105*, 11929−11932.